Investigation of giant dipole resonances in heavy deformed nuclei with an extended quantum molecular dynamics model

S. S. Wang (王闪闪),[1,2] Y. G. Ma (马余刚),[1,3,*] X. G. Cao (曹喜光),[1] W. B. He (何万兵),[4]
H. Y. Kong (孔海云),[1,2] and C. W. Ma (马春旺)[5]

[1]*Shanghai Institute of Applied Physics, Chinese Academy of Sciences, Shanghai 201800, China*
[2]*University of Chinese Academy of Sciences, Beijing 100049, China*
[3]*Shanghai Tech University, Shanghai 200031, China*
[4]*Institute of Modern Physics, Fudan University, Shanghai 200433, China*
[5]*Institute of Particle and Nuclear Physics, Henan Normal University, Xinxiang 453007, China*

(Received 19 January 2017; revised manuscript received 7 March 2017; published 18 May 2017)

The deformation evolution of giant dipole resonance (GDR), in the chains of Sm and Nd isotopes, are investigated in the framework of an extended quantum molecular dynamics (EQMD) model. The mass number dependence of resonance peak position (E_m) in the major and minor axis directions of deformed nuclei as well as the difference ΔE_m between them are described in detail. The correlation between the splitting ($\Delta E_m/\bar{E}_m$) of the GDR spectra and the deformation (β_2) is further studied. The results confirm that $\Delta E_m/\bar{E}_m$ is proportional to β_2. By comparing the calculation with the experimental data on photon absorption cross section σ_γ, it shows that the EQMD model can quite well reproduce the shape of GDR spectra from spherical to prolate shape. The GDR shapes in ^{134}Sm, ^{136}Sm, ^{138}Sm, ^{130}Nd, ^{132}Nd, and ^{134}Nd are also predicted. In addition, the symmetry energy coefficient ($E_{\rm sym}$) dependence of GDR spectra of ^{150}Nd is also discussed. It is found that the calculated GDR spectrum in the EQMD model is perfectly consistent with the experimental results when $E_{\rm sym}$ equals 32 MeV.

DOI: 10.1103/PhysRevC.95.054615

I. INTRODUCTION

Giant dipole resonance (GDR) is the most prominent characteristic in the excitation spectrum for all nuclei (except for deuterons) in the nuclide chart, which has been regarded as a specific probe for measuring the shape of a nucleus. Owing to this fact, there is increasing interest in applications to the dynamics of exotic nuclei. The relationship of the geometrical and dynamical symmetries of α-clustering configuration with the number and centroid energies of peaks in the GDR spectra has been discussed in Refs. [1,2]. The evolution of GDR with neutron excess for the neutron-rich oxygen isotopes has been systematically measured in Ref. [3]. Additionally, because deformation effects in GDR spectrum were first seen more than 50 yr ago in terms of a double-humped photon cross section peak [4], it has been well established that the GDR peak is split into two components owing to the different frequencies of dipole oscillation along the major axis and minor axis in heavy deformed nuclei [5–8].

A deformed nucleus provides an interesting testing ground because there is a strong interplay between the structure of the GDR and the ground-state deformation [9]. Many works have been done both theoretically [10–17] and experimentally [5,6,18–21] to investigate the effects of deformation in GDRs in heavy deformed nuclei. Most of the studies of the GDRs in deformed nuclei have been focused on the dependence of the width at half maximum, peak position, and strength of dipole resonance on deformation.

Various microscopic methods have been employed to investigate the GDRs of deformed nuclei such as the random-phase approximation approach [10–13,22,23], time-dependent Skyrme-Hartree-Fock method [14,16], time-dependent density functional theory [24], and phonon damping model [25]. The excitation of the GDRs in the experiment is induced by inelastic scattering [26–28], photoabsorption [18–20,29], γ decay [30], and so on. However, few studies have been conducted about the GDRs in heavy deformed nuclei using a dynamical method.

In this article, the extended quantum molecular dynamics (EQMD) model [31] has been applied to study the GDRs in Sm and Nd isotopes. The initial ground-state deformed nuclei are boosted by imposing a dipole excitation to obtain the GDR spectra. Both the brief introduction of the EQMD model and the methods of calculating GDR spectrum are shown in Sec. II. To check the reliability of our calculation, the evolution of dipole moments in coordinator space and in momentum space versus time are exhibited in Sec. III. The discussions, including the mass number dependence of resonance width along the major and minor axes, the comparison of the calculations with the experimental measurement, and the effect of symmetry energy coefficient on GDR are also carried out in this section. Finally, Sec. IV gives the summary.

II. MODEL AND FORMALISM

A. Introduction of the EQMD model

The EQMD model was developed from the quantum molecular dynamics (QMD) model [32–35] by adding the so-called Pauli potential to the effective interaction and treating the width of Gaussian wave packets for each nucleon as a dynamical variable. The initial ground-state nuclei are obtained at their minimum energy states, which are sufficiently stable so that they can be considered as at the real ground

*ygma@sinap.ac.cn

states [31,36,37]. Thanks to the advantage, the EQMD model has been successfully applied to study the GDR of the α-clustering nuclei [1,2]. In this article, we use the EQMD model to investigate the GDRs in heavy deformed nuclei. A brief introduction of the EQMD model follows.

In the model, the total wave function of the system is treated as a direct product of Gaussian wave packets of all nucleons [31],

$$\Psi = \prod_i \varphi(\mathbf{r}_i), \tag{1}$$

$$\varphi(\mathbf{r}_i) = \left(\frac{\nu_i + \nu_i^*}{2\pi}\right)^{3/4} \exp\left[-\frac{\nu_i}{2}(\mathbf{r}_i - \mathbf{R}_i)^2 + \frac{i}{\hbar}\mathbf{P}_i \cdot \mathbf{r}_i\right], \tag{2}$$

where $\mathbf{R}_i$ and $\mathbf{P}_i$ are the centers of position and momentum of the ith wave packet, respectively. The Gaussian width ν_i is introduced using a complex as

$$\nu_i \equiv \frac{1}{\lambda_i} + i\delta_i, \tag{3}$$

where λ_i and δ_i denote the real and the imaginary parts. They are dynamical variables in the process of initialization.

The effective interaction contains Skyrme, Coulomb, and symmetry potential, as well as the Pauli potential:

$$H_{\text{int}} = H_{\text{Skyrme}} + H_{\text{Coulomb}} + H_{\text{symmetry}} + H_{\text{Pauli}}. \tag{4}$$

The simplest form is used for the Skyrme interaction,

$$H_{\text{Skyrme}} = \frac{\alpha}{2\rho_0}\int \rho^2(\mathbf{r})d^3r + \frac{\beta}{(\gamma+1)\rho_0^\gamma}\int \rho^{\gamma+1}(\mathbf{r})d^3r, \tag{5}$$

with $\alpha = -124.3$ MeV, $\beta = 70.5$ MeV, and $\gamma = 2$. They are obtained by fitting the ground-state properties of the finite nuclei.

For the Pauli potential, a very simple form is applied by introducing a phenomenological repulsive potential which inhibits nucleons of the same spin S and isospin T to come close to each other in the phase space,

$$H_{\text{Pauli}} = \frac{c_p}{2}\sum_i (f_i - f_0)^\mu \theta(f_i - f_0), \tag{6}$$

where c_p denotes the strength of the Pauli potential, which equals 15 MeV. For the other two parameters, we take $f_0 = 1.0$ and $\mu = 1.3$. f_i is the overlap of a nucleon i with the same spin S and isospin T as

$$f_i \equiv \sum_j \delta(S_i, S_j)\delta(T_i, T_j)|\langle\varphi_i|\varphi_j\rangle|^2, \tag{7}$$

and θ is the unit step function.

The symmetry potential is written as

$$H_{\text{symmetry}} = \frac{E_{\text{sym}}}{2\rho_0}\sum_{i,j\neq i}\int [2\delta(T_i, T_j) - 1]\rho_i(\mathbf{r})\rho_j(\mathbf{r})d^3r, \tag{8}$$

where E_{sym} is the symmetry energy coefficient.

The stability of nuclei in the model description is very important to study the structure effects of nuclei, for example deformation structure. In the EQMD model, the energy-minimum state is considered as the ground state of initial nuclei. At the beginning, a random configuration is given to a nucleus. Then the initial ground-state nuclei are obtained by solving the damped equations of motion as

$$\begin{aligned} \dot{\mathbf{R}}_i &= \frac{\partial H}{\partial \mathbf{P}_i} + \mu_{\mathbf{R}}\frac{\partial H}{\partial \mathbf{R}_i}, \quad \dot{\mathbf{P}}_i = -\frac{\partial H}{\partial \mathbf{R}_i} + \mu_{\mathbf{P}}\frac{\partial H}{\partial \mathbf{P}_i}, \\ \frac{3\hbar}{4}\dot{\lambda}_i &= -\frac{\partial H}{\partial \delta_i} + \mu_\lambda\frac{\partial H}{\partial \lambda_i}, \quad \frac{3\hbar}{4}\dot{\delta}_i = \frac{\partial H}{\partial \lambda_i} + \mu_\delta\frac{\partial H}{\partial \delta_i}, \end{aligned} \tag{9}$$

where $\mu_{\mathbf{R}}$, $\mu_{\mathbf{P}}$, μ_λ, and μ_δ are damping coefficients. With negative values of these coefficients, the system goes to its (local) energy minimum point:

$$\begin{aligned} \frac{dH}{dt} &= \sum_i\left[\frac{\partial H}{\partial \mathbf{R}_i}\dot{\mathbf{R}}_i + \frac{\partial H}{\partial \mathbf{P}_i}\dot{\mathbf{P}}_i + \frac{\partial H}{\partial \lambda_i}\dot{\lambda}_i + \frac{\partial H}{\partial \delta_i}\dot{\delta}_i\right] \\ &= \sum_i\left[\mu_{\mathbf{R}}\left(\frac{\partial H}{\partial \mathbf{R}_i}\right)^2 + \mu_{\mathbf{P}}\left(\frac{\partial H}{\partial \mathbf{P}_i}\right)^2 + \frac{4\mu_\lambda}{3\hbar}\left(\frac{\partial H}{\partial \lambda_i}\right)^2 \right. \\ &\quad \left. + \frac{4\mu_\delta}{3\hbar}\left(\frac{\partial H}{\partial \delta_i}\right)^2\right] \leqslant 0. \end{aligned} \tag{10}$$

B. Giant dipole resonance in deformed nuclei

To study the GDRs of the deformed nuclei that have an ellipsoidal shape in the framework of EQMD model, we first need to obtain the phase-space information of the ground-state deformed nuclei, which have been proven and measured in the experiments. Nevertheless, the fact is that not all of the phase-space distributions of the initial nuclei obtained from initialization with the EQMD model are ellipsoidal; it is indispensable to select the deformed nuclei from all initial nuclei, whose deformations are consistent with the experimental measurements. Here, the initial deformed nuclei are selected by comparing the calculated deformation parameter β_2 with the experimental data. β_2 is a parameter linked through the symmetry-axis radius R_x and the radius R_0 of the spherical nucleus with the same mass in accordance with the following relationship:

$$\beta_2 = \sqrt{\frac{4\pi}{5}}\frac{R_x - R_0}{R_0}. \tag{11}$$

Note that in the EQMD model, R_0 is taken as the root-mean-squared radius.

According to the macroscopic description of GDR given by the Goldhaber-Teller model [38], the GDR is considered as a coherent dipole oscillation of the bulk of protons and neutrons along the opposite direction in an excited nucleus. In this work, the initial nucleus is triggered by means of giving a displacement between protons and nucleons at $t = 0$ fm/c, and then a dipole excitation is triggered and evolved with time. The dipole moments of the system in coordinator space $D_G(t)$ and in momentum space $K_G(t)$ are defined, respectively, as [1,2,39–41]

$$D_G(t) = \frac{NZ}{A}[R_Z(t) - R_N(t)], \tag{12}$$

$$K_G(t) = \frac{NZ}{A\hbar}\left[\frac{P_Z(t)}{Z} - \frac{P_N(t)}{N}\right], \tag{13}$$

where $R_Z(t)[P_Z(t)]$ and $R_N(t)[P_N(t)]$ are the centers of motion of the protons and neutrons in coordinate (momentum) space, respectively.

The strength of the dipole resonance of the system at energy E_γ can be derived from the dipole moments $D_G(t)$, i.e.,

$$\frac{dP}{dE_\gamma} = \frac{2e^2}{3\pi\hbar c^3 E_\gamma}|D''(\omega)|^2, \tag{14}$$

where $\frac{dP}{dE_\gamma}$ can be interpreted as the γ emission probability. $D''(\omega)$ is from the the Fourier transform of the second derivative of $D_G(t)$ with respect to time; i.e.,

$$D''(\omega) = \int_{t_0}^{t_{\max}} D''_G(t)e^{i\omega t}dt. \tag{15}$$

It needs to be noted that the evolution time can not be infinite long in the realistic calculation and the Fourier transform in the infinite time range is not reasonable owing to the GDR spectrum having the natural width. Moreover, the different final states affect only the width of GDR spectra, which determine the effective width of the Fourier transform in Eq. (15). However, they do not affect the peak position (E_m) of the resonance maximum. So we take $t_{\max} = 300$ fm/c as the final state in this work.

The peak of the GDRs in deformed nuclei splits two parts, while there is only one single peak for the spherical nuclei. In the EQMD model, we calculate the GDRs along the x and z axes, respectively. In analogy to the superposition of two noninterfering Lorentz lines for statically deformed nuclei (the lower-energy line corresponds to oscillations along the major axis and the higher-energy line along the minor) for fitting the experimental data [6], we take the method of the superposition of two GDR spectra to gain the total resonance strength in a deformed nucleus. The formula is given as

$$\frac{dP}{dE_\gamma} = \sum_{i=1}^{2} \frac{\left(\frac{dP}{dE_\gamma}\right)_{mi}}{1 + \frac{(E_\gamma^2 - E_{mi}^2)^2}{E_{mi}^2\Gamma_i^2}}, \tag{16}$$

where $(\frac{dP}{dE_\gamma})_m$ is the resonance strength maximum; E_m is the peak position of the resonance maximum, Γ_i is the resonance width at half-maximum, and $i = 1,2$ correspond to the x- and z-axis resonance components of the deformed nucleus. Note that the above three parameters are all obtained by fitting the single GDR spectrum along two axis directions with the Gaussian function, and the x axis corresponds to the major axis, and the z axis is the minor axis of the nucleus in our calculation.

III. RESULTS AND DISCUSSION

Nuclei in the region of mass number $Z = 60$ (Nd) and $Z = 62$ (Sm) display a transition from spherical, at the neutron number N close to 82, to prolate ellipsoidal shape. Considering this, the chains of Nd and Sm isotopes are used to study the deformation dependence of GDR spectra in the framework of the EQMD model. The experimental data of photon absorption cross sections σ_γ in the GDR range are extracted from Ref. [19] for Sm isotopes and from Ref. [20] for Nd isotopes.

TABLE I. The deformation parameter β_2, the experimental data are from Ref. [42] and the calculation are based on Eq. (11).

Nuclei	β_2 Exp. [42]	β_2 Calcu.
^{130}Nd	0.37 ± 0.09	0.3586 ± 0.0109
^{132}Nd	0.349 ± 0.03	0.3485 ± 0.0139
^{134}Nd	0.249 ± 0.025	0.2558 ± 0.007
^{142}Nd	0.0917 ± 0.001	0.0941 ± 0.0136
^{144}Nd	0.1237 ± 0.0006	0.1019 ± 0.0047
^{146}Nd	0.1524 ± 0.0025	0.1497 ± 0.0182
^{148}Nd	0.2013 ± 0.0037	0.2133 ± 0.0035
^{150}Nd	0.2853 ± 0.0021	0.2733 ± 0.0173
^{134}Sm	0.366 ± 0.026	0.3576 ± 0.0053
^{136}Sm	0.293 ± 0.015	0.2846 ± 0.0116
^{138}Sm	0.208 ± 0.017	0.2091 ± 0.0169
^{144}Sm	0.0874 ± 0.001	0.0869 ± 0.0087
^{148}Sm	0.1423 ± 0.003	0.1547 ± 0.0113
^{150}Sm	0.1931 ± 0.0021	0.1861 ± 0.0097
^{152}Sm	0.3064 ± 0.0027	0.315 ± 0.0157
^{154}Sm	0.341 ± 0.002	0.3443 ± 0.0072

The deformation parameter β_2 as one main parameter of describing the deformed nuclei is treated as a probe to select the ground deformed nuclei from all initial nuclei in this article. In Table I, the β_2 in the chains of Nd and Sm isotopes are shown, including the experimental data from Ref. [42] and the calculation based on Eq. (11). The statistical errors are also attached for each nucleus in the table. From the table, we can find the β_2 of our calculations are very close to the experimental values.

In this work, the collective motion is divided into two directions along the x and z axes. The initial-state wave function of the system is boosted by means of imposing a dipole excitation at $t = 0$ fm/c. The time evolution of the dipole moments of Sm isotopes in coordinator space (D_G) and in momentum space (K_G) are shown in Figs. 1(a) and 1(b), respectively. It is found that all the dipole oscillations are symmetrical around $D_G(K_G) = 0$, except for that close to the initial time. The resonance frequencies along the x-axis direction are lower than those in z-axis direction. That is why a deformed nucleus has two splitting peaks in its GDR spectrum. The same situation occurs in the Nd isotopes.

The total GDR spectra are obtained from the superposition of two GDR spectra along the x and z axes by Eq. (16). The peak position (E_m) of the resonance maximum and the resonance width (Γ) are two indispensable parameters to get the total resonance strength. That is one reason to show the mass evolution of E_m of GDRs in the chains of Sm and Nd isotopes in Fig. 2(a). The open symbols denote the E_m along the x axis, which corresponds to the major axis of a deformed nucleus. The solid symbols represent the E_m in the z-axis direction, corresponding to the minor axis of the deformed nucleus. It can be seen that with the increasing of A, the resonance E_m in the z-axis direction first decreases and then trends to increase. On the contrary, the resonance E_m along the x-axis direction gradually increases with the increasing of A until the mass number equals to 142 in the chain of Nd

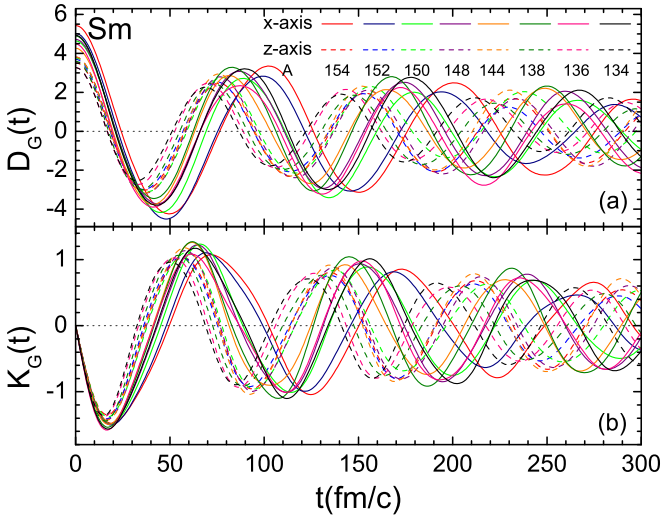

FIG. 1. The time evolution of the dipole moments in coordinator space (a) and in momentum space (b) for the chain of Sm isotopes computed using Eqs. (12) and (13) with the EQMD model, respectively. The solid lines denote the D_G (K_G) along the x axis and the dashed lines correspond to that along the z axis. Dotted lines in (a) and (b) (dark gray line) represent D_G (K_G) = 0.

isotopes and equals to 144 in the chain of Sm isotopes and then gradually decreases. It is necessary to note that ^{142}Nd and ^{144}Sm are magic nuclei. From Fig. 2(b), it can be easily seen that the distance ΔE_m between the resonance E_m along

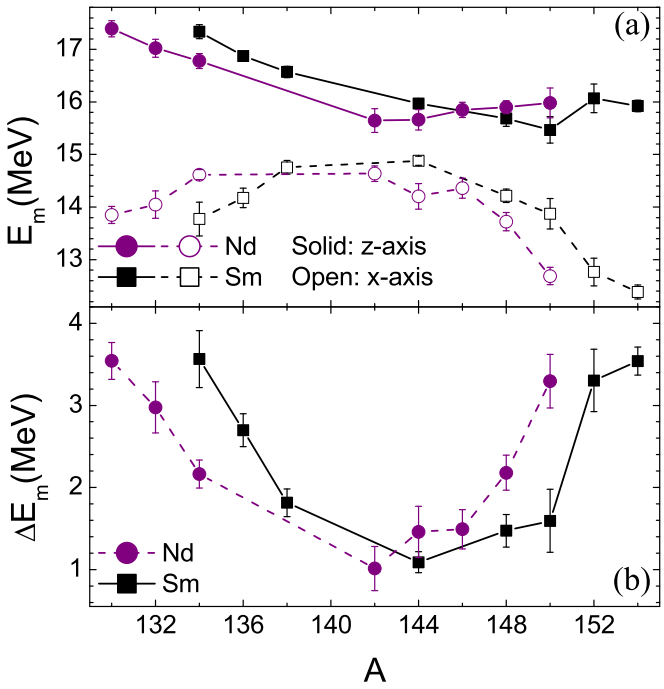

FIG. 2. (a) The peak position (E_m) of GDRs along the x (open symbols) and z axes (solid symbols) in Sm (black squares) and Nd isotopes (purple circles), respectively. (b) The mass dependence of the difference (ΔE_m) between two GDR peak positions in two decomposed directions for each Sm (black squares) and Nd (purple circles) isotope.

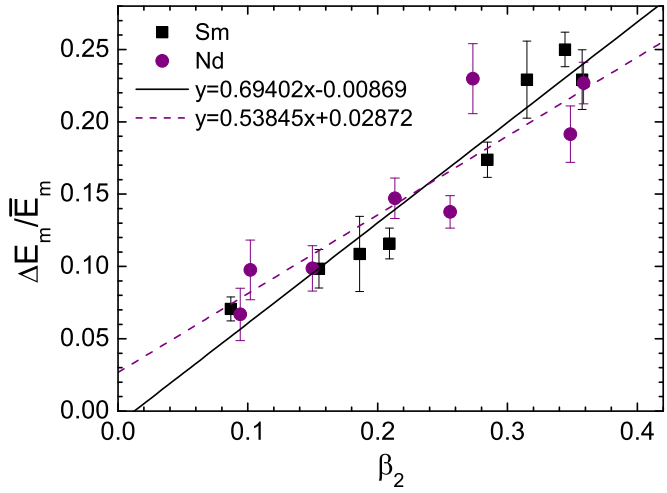

FIG. 3. The correlation between $\Delta E_m/\bar{E}_m$ and deformation parameter β_2 which is obtained by Eq. (11). Lines are the fitting results. Black squares and purple circles denote the data in the chain of Sm and Nd isotopes, respectively.

two axes first decreases with the increasing of A and then increases, which can also be described as the less the deformed a nucleus is, the closer the two resonance E_m's are. It confirms that the splitting peak in the deformed nuclei results from the deformation structure of the nuclei.

Furthermore, the correlation between $\Delta E_m/\bar{E}_m$ and deformation parameter β_2 is shown in Fig. 3. Note that $\bar{E}_m$ is the mean resonance energy. Black squares denote the data of Sm isotopes and purple circles denote that of Nd isotopes. β_2 is computed based on Eq. (11). Both solid and dashed lines are the linear fitting results. The fitting parameters also are listed in the figure. For the chain of Sm isotopes, the relationship between $\Delta E_m/\bar{E}_m$ and the deformation parameter is $\Delta E_m/\bar{E}_m = 0.694\,02\beta_2 - 0.008\,69$; for the chain of Nd isotopes, the relationship is $\Delta E_m/\bar{E}_m = 0.538\,45\beta_2 + 0.028\,72$. It also confirms that the splitting between the x- and z-axis modes of the deformed nuclei is proportional to the deformation, which has been described in detail in Ref. [8].

In Fig. 4, dipole strengths based on Eq. (14) for the separate modes in the framework of the EQMD model are plotted with different lines. It can be seen that the oscillations along the x axis which denote the major axis of symmetry correspond to the lower-energy state, and that along the y axis and z axis which denote the minor axis of symmetry correspond to the higher-energy state. For ^{142}Nd and ^{144}Sm, which are magic nuclei, their resonance peaks along the three axes are so close that the total GDR spectrum has a single hump. However, for ^{130}Nd, ^{150}Nd, ^{134}Sm, and ^{154}Sm, the resonance peaks along the major axis are much smaller than those along the minor axis, and the resonance spectra along the y axis and z axis nearly overlap. Consequently, in an ellipsoid-deformed nucleus, the total GDR spectrum has two humps. For the resonance spectra along the y-axis direction, it is not perfectly identical to the one along the z axis, which mostly results from the shape fluctuation of the initial deformed nucleus in EQMD model.

The deformation evolution of the total GDR spectra along the x- and z-axis directions in Sm and Nd isotopes are plotted

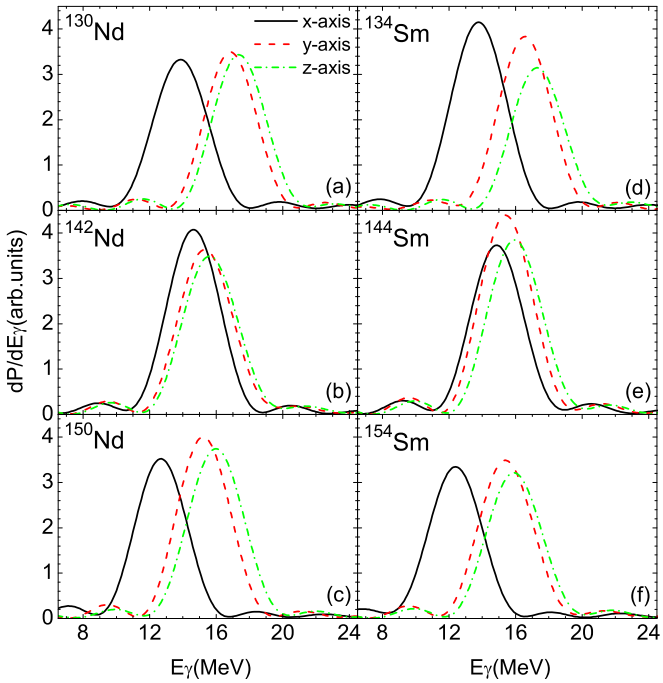

FIG. 4. Dipole strengths in the Nd isotopes and Sm isotopes based on Eq. (14). Solid lines denote modes along the x-axis direction, dashed lines denote modes along the y-axis direction, and dash-dotted lines denote modes along the z-axis direction.

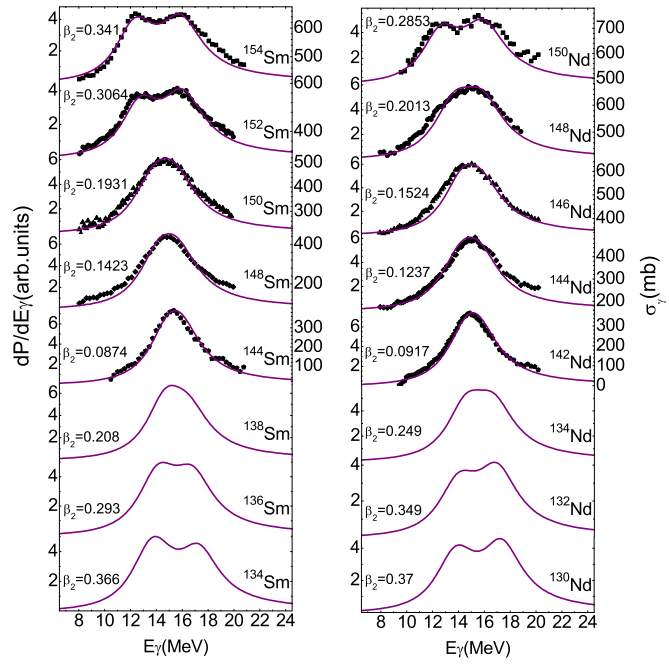

FIG. 5. The GDR spectra in the isotopic chain of Sm (A = 134–154) and Nd isotopes (A = 130–150). The lines denote the calculation in the EQMD model (scaled by the left y axis). Dots represent the experimental data (photon absorption cross sections σ_γ, scaled by the right y axis). The deformation parameter β_2 from Ref. [42] is displayed in each panel.

in Fig. 5, where the deformation parameter β_2 from Ref. [42] is inserted in each panel. The lines denote our calculation by Eq. (16) in the framework of the EQMD model, scaled by the left y axis and the dots denote the experimental data, scaled by the right y axis.

It needs to be pointed out that the photon absorption cross sections σ_γ in the GDR range for ^{134}Sm, ^{136}Sm, ^{138}Sm, ^{130}Nd, ^{132}Nd, and ^{134}Nd are unknown in the experiment so far. We also give their total GDR spectra by the superposition of two single GDR spectrum along the x- and z-axis directions, according to Eq. (16). From Fig. 5, one can see that the calculated GDRs can perfectly reproduce the shape of the GDR spectra. For example, the GDR spectra have two distinctly splitting peaks in the region of strongly deformed nuclei, such as in ^{154}Sm, ^{152}Sm, ^{136}Sm, ^{134}Sm, ^{150}Nd, ^{132}Nd, and ^{130}Nd, while there is only one maximum value when the deformation of a nucleus is very small, especially for the magic nuclei ^{144}Sm and ^{142}Nd. Further, with the decreasing of the deformation of nuclei, the GDR width also decreases, which occurs in both Sm and Nd isotopes. All of these characteristics above have been observed in the experiment. Additionally, it can also be seen that all of the peak position, for the isotopic chain of Sm (A = 142–154) and Nd (A = 140–150) isotopes, is well consistent with the measured data. Therefore, the results not only confirm the reliability of the methods and the model to study the GDR in deformed nuclei, but also predict the shapes of GDR spectra in Sm (A = 134,136,138) and Nd (A = 130,132,134) isotopes, which is possible to be verified by experiments.

The dependence of the GDRs on symmetry energy coefficient ($E_{\rm sym}$) is also discussed for the heavy deformed nucleus of ^{150}Nd in the EQMD model. The results are shown in Fig. 6. The dots represent the measured data from the experiment, which are the photon absorption cross sections σ_γ in the GDR range, scaled by the right y axis. The calculations are plotted as the different lines corresponding to different $E_{\rm sym}$, scaled by the left y axis. From the figure, it is cleanly seen that with

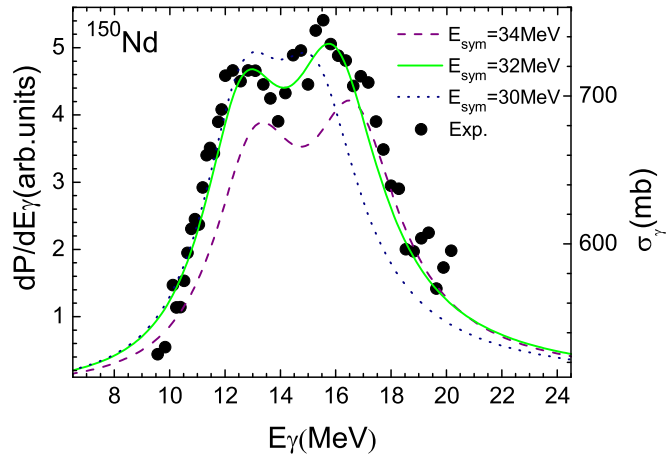

FIG. 6. The dependence of the GDR spectra on symmetry energy coefficient ($E_{\rm sym}$) in heavy deformed nuclei ^{150}Nd. Dots show the experimental data (photon absorption cross sections σ_γ, scaled by the right y axis). The dashed line, solid line, and dotted lines correspond to the calculating results (scaled by the left y axis) at $E_{\rm sym}$ equal to 34, 32, and 30 MeV, respectively.

the increasing of $E_{\rm sym}$ from 30 to 34 MeV, the GDR spectra of the system have the obvious trend of moving to the right; i.e., the energy position of GDR is governed by the symmetry energy. Meanwhile, one can find that the calculation is well consistent with the experimental value at $E_{\rm sym} = 32$ MeV, which demonstrates that 32 MeV is the best choice for the symmetry energy coefficient to investigate the GDRs in heavy deformed nuclei in the framework of the EQMD model.

IV. SUMMARY AND OUTLOOK

In summary, the deformation evolution of giant dipole resonance, in the isotopic chains of Sm and Nd, has been systematically studied under the framework of an extended quantum molecular dynamics model. The discussions are conducted about the mass dependence of resonance peak position (E_m) in the major and minor axis directions as well as the difference ΔE_m between them, respectively. The ΔE_m between the two resonance E_m's first decreases with the increasing of A and then trends to increase. It confirms that ΔE_m is extremely sensitive to the deformation of a nucleus. Moreover, the correlation between $\Delta E_m/\bar{E}_m$ and the deformation parameter (β_2) is considered. For the isotopic chain of Sm, $\Delta E_m/\bar{E}_m = 0.694\,02\beta_2 - 0.008\,69$, and for the isotopic chain of Nd, $\Delta E_m/\bar{E}_m = 0.538\,45\beta_2 + 0.028\,72$. It further confirms that the splitting of the GDR spectra along the major axis and the minor axis is proportional to the deformation of a nucleus. Additionally, by comparing the calculation with the experimental data of photon absorption cross section σ_γ, the results show that the EQMD model can perfectly reproduce the shape of the GDR spectra. The GDR spectra in ^{134}Sm, ^{136}Sm, ^{138}Sm, ^{130}Nd, ^{132}Nd, and ^{134}Nd are also predicted in detail. Finally, the dependence of GDR spectra of ^{150}Nd on symmetry energy coefficient ($E_{\rm sym}$) are considered. The results demonstrate that the calculation is well consistent with the experimental results at $E_{\rm sym} = 32$ MeV. It suggests that the EQMD model can be used to study the configuration structure of deformed nuclei.

In light of the success for describing the deformed GDR by the EQMD model, it is expected that it could also be applied to treat the pygmy dipole resonance (PDR), which can be considered as the oscillation between the weakly bound neutron skin and the isospin neutral proton-neutron core for neutron-rich nuclei. Previously, a traditional QMD model has shown its capability to investigate PDR and GDR in Ni isotopes by Coulomb excitation [40]; it is naturally expected that the EQMD can do as good a job for the PDR study because more reasonable ground-state nuclei could be obtained in the EQMD initialization, in contrast to the traditional QMD initialization.

ACKNOWLEDGMENTS

This work is supported by the National Natural Science Foundation of China under Contracts No. 11421505, No. 11305239, and No. 11220101005, the Major State Basic Research Development Program in China under Contract No. 2014CB845401, the Key Research Program of Frontier Sciences of the CAS under Grant No. QYZDJ-SSW-SLH002, the Strategic Priority Research Program of the Chinese Academy of Sciences under Grant No. XDB16, the Youth Innovation Promotion Association of CAS under Grant No. 2017309, the Program for Science and Technology Innovation Talents in Universities of Henan Province under Grant No. 13HASTIT046, and the Natural Science Foundation in Henan Province under Grant No. 162300410179.

[1] W. B. He, Y. G. Ma, X. G. Cao, X. Z. Cai, and G. Q. Zhang, Phys. Rev. Lett. **113**, 032506 (2014).
[2] W. B. He, Y. G. Ma, X. G. Cao, X. Z. Cai, and G. Q. Zhang, Phys. Rev. C **94**, 014301 (2016).
[3] A. Leistenschneider, T. Aumann, K. Boretzky *et al.*, Phys. Rev. Lett. **86**, 5442 (2001).
[4] E. G. Fuller and E. Hayward, Nucl. Phys. **30**, 613 (1962).
[5] B. S. Ishkhanov and S. Yu. Troshchiev, Moscow Univ. Phys. Bull. (Engl. Transl.) **66**, 325 (2011).
[6] B. L. Herman and S. C. Fultz, Rev. Mod. Phys. **47**, 713 (1975).
[7] W. Greiner and J. A. Maruhn, *Nuclear Models* (Springer, Berlin, Germany, 1996).
[8] A. Bohr and B. Mottelson, Nucl. Struct. **2**, 1 (1998).
[9] M. Danos, Nucl. Phys. **5**, 23 (1958).
[10] M. Martini, S. Péru, S. Hilaire, S. Goriely, and F. Lechaftois, Phys. Rev. C **94**, 014304 (2016).
[11] S. Péru, G. Gosselin, M. Martini, M. Dupuis, S. Hilaire, and J.-C. Devaux, Phys. Rev. C **83**, 014314 (2011).
[12] K. Yoshida and T. Nakatsukasa, Phys. Rev. C **88**, 034309 (2013).
[13] K. Yoshida and T. Nakatsukasa, Phys. Rev. C **83**, 021304(R) (2011).
[14] J. A. Maruhn, P. G. Reinhard, P. D. Stevenson, J. R. Stone, and M. R. Strayer, Phys. Rev. C **71**, 064328 (2005).
[15] B. S. Ishkhanov *et al.*, Phys. Part. Nucl. **38**, 232 (2007).
[16] S. Fracasso, E. B. Suckling, and P. D. Stevenson, Phys. Rev. C **86**, 044303 (2012).
[17] J. Tian and W. Ye, Nucl. Sci. Tech. **27**, 145 (2016).
[18] V. M. Masur and and L. M. Mel'nikova, Phys. Part. Nucl. **37**, 923 (2006).
[19] P. Carlos, H. Beil, R. Bergere *et al.*, Nucl. Phys. A **225**, 171 (1974).
[20] P. Carlos, H. Beil, R. Bergere *et al.*, Nucl. Phys. A **172**, 437 (1971).
[21] D. Pandit, B. Dey, D. Mondal *et al.*, Phys. Rev. C **87**, 044325 (2013).
[22] W. Kleinig, V. O. Nesterenko, J. Kvasil, P.-G. Reinhard, and P. Vesely, Phys. Rev. C **78**, 044313 (2008).
[23] J. Liang, L.-G. Cao, and Z.-Y. Ma, Phys. Rev. C **75**, 054320 (2007).
[24] I. Stetcu, A. Bulgac, P. Magierski, and K. J. Roche, Phys. Rev. C **84**, 051309(R) (2011).
[25] N. D. Dang, K. Tanabe, and A. Arima, Nucl. Phys. A **645**, 536 (1999).

[26] T. Peach, U. Garg, Y. K. Gupta *et al.*, Phys. Rev. C **93**, 064325 (2016).
[27] D. H. Youngblood, J. M. Moss, C. M. Rozsa *et al.*, Phys. Rev. C **13**, 994 (1976).
[28] M. Itoh, H. Sakaguchi, M. Uchida *et al.*, Phys. Lett. B **549**, 58 (2002).
[29] V. A. Plujko, R. Capote, and O. M. Gorbachenko, At. Data Nucl. Data Tables **97**, 567 (2011).
[30] J. H. Gundlach, K. A. Snover, J. A. Behr, C. A. Gossett, M. Kicinska-Habior, and K. T. Lesko, Phys. Rev. Lett. **65**, 2523 (1990).
[31] T. Maruyama, K. Niita, and A. Iwamoto, Phys. Rev. C **53**, 297 (1996).
[32] J. Aichelin and H. Stöcker, Phys. Lett. B **176**, 14 (1986).
[33] C. Hartnack, R. K. Puri, J. Aichelin *et al.*, Eur. Phys. J. A **1**, 151 (1998).
[34] Z. Q. Feng, Nucl. Sci. Tech. **26**, S20512 (2015).
[35] J. Chen, Z. Q. Feng, J. S. Wang *et al.*, Nucl. Sci. Tech. **27**, 73 (2016).
[36] S. S. Wang, X. G. Cao, T. L. Zhang *et al.*, Nucl. Phys. Rev. (in Chinese) **32**, 24 (2015).
[37] W. B. He, X. G. Cao, Y. G. Ma *et al.*, Nucl. Tech. (in Chinese) **37**, 100511 (2014).
[38] M. Goldhaber and E. Teller, Phys. Rev. **74**, 1046 (1948).
[39] H. L. Wu, W. D. Tian, Y. G. Ma *et al.*, Phys. Rev. C **81**, 047602 (2010).
[40] C. Tao, Y. G. Ma, G. Q. Zhang, X. G. Cao, D. Q. Fang, and H. W. Wang, Phys. Rev. C **87**, 014621 (2013).
[41] V. Baran, M. Cabibbo, M. Colonna *et al.*, Nucl. Phys. A **679**, 373 (2001).
[42] S. Raman, C. W. Nestor Jr., and P. Tikkanen, At. Data Nucl. Data Tables **78**, 1 (2001).